Journal of Bioscience and Bioengineering
VOL. 127 No. 2, 129–137, 2019

www.elsevier.com/locate/jbiosc

Purification and characterization of arginine deiminase from *Pseudomonas putida*: Structural insights of the differential affinities of L-arginine analogues

Mahesh D. Patil,[1] Vijay P. Rathod,[2] Umesh R. Bihade,[1] and Uttam Chand Banerjee[1,*]

Department of Pharmaceutical Technology (Biotechnology), National Institute of Pharmaceutical Education and Research, Sector 67, S.A.S. Nagar, Punjab 160062, India[1] *and Department of Pharmacoinformatics, National Institute of Pharmaceutical Education and Research, Sector 67, S.A.S. Nagar, Punjab 160062, India*[2]

Received 14 May 2018; accepted 23 July 2018
Available online 22 August 2018

Arginine deiminase (ADI) from *Pseudomonas putida* was purified using ammonium sulphate precipitation, anion exchange and hydrophobic interaction chromatography. Influence of various chemical compounds (metal ions, reducing agents, sulphydryl agents, and surfactants) on the catalytic activity of ADI was determined was evaluated on the purified ADI. The enzyme displayed high sensitivity towards thiol binding metal ions, chemicals acting on sulfhydryl group, and most of the surfactants. Substrate specificity studies exhibited that among the eight substrate analogues tested, canavanine had the highest affinity for ADI, followed by D-arginine and guanidine. Canavanine decreased the ADI activity up to 50% at its lowest concentration tested (10 mM), while D-arginine decreased the ADI activity up to ~4% at its highest tested concentration (200 mM). Differential affinities of the structural analogues of arginine towards ADI were further studied by molecular modeling methods, which included homology modeling, molecular docking and molecular dynamic simulations. The molecular docking studies revealed the critical importance of residues Arg 243, Asp 166, Asp 280, Gly 299 and His 278. RMSDs for protein-ligand complexes were within a range of 1–3 Å, suggesting that the complexes were stable throughout the molecular dynamic simulation. The formation of strong hydrogen bonds by residues Asn 160, Asp166, Arg 185, Arg243, Asp280 and Gly 399 in L-arginine were preserved in the case of D-arginine and canavanine and was responsible for higher affinity towards ADI. Calculations of the substrate binding energies revealed that binding energies ΔG_{bind} and ΔG_{vdw} play a critical role for the differential affinities of various substrate analogues towards *P. putida* ADI.

[**Key words:** Arginine deiminase; Substrate affinity; Molecular docking; Molecular dynamics; Homology modeling]

Arginine deiminase (ADI) is a potential anti-tumor modality that has been granted an orphan drug status by U.S. Food and Drug Administration for the treatment of hepatocellular carcinomas and melanomas (1). ADI-mediated conversion of arginine to citrulline is also a potential approach for the production of citrulline (2,3). ADI from *Pseudomonas putida* KT2440 has not been previously demonstrated for its uses and it is very important to purify this enzyme for its further characterization. Due to its high anti-tumor potentials, ADI from different bacterial genera have been characterized. Major examples include such as *Lactobacillus*, *Mycoplasma*, *Lactococcus*, *Pseudomonas* (4). During the recent years, much attention has been paid to ADI from *Pseudomonas* genus. Crystal structure of *Pseudomonas aeruginosa* has been determined by the multi-wavelength anomalous diffraction method at 2.45 Å resolution (5). Furthermore, a substrate-induced conformational transition, playing an important role in regulation of ADI activity, also has been discovered. In addition, plausible mechanisms of active site catalysis and other structural insights have been demonstrated for *P. aeruginosa* ADI (6). Recently, a new strain of *Pseudomonas* genera, *Pseudomonas plecoglossicida* CGMCC2039, producing highly active ADI has been isolated (7). Furthermore, *P. plecoglossicida* CGMCC2039 ADI enzyme properties have been improved by rational design and directed evolution approaches (8–10).

Despite of its high potential, ADI from *P. putida* has not been well explored by scientific community and much is still elusive about the molecular mechanisms of its enzymatic properties. In view of the notion that ADI from *P. putida* KT2440 can be a potential anti-tumor modality (11), we report the structural insights of the enzymatic properties, including the key interactions playing important role in ligand–enzyme complex formation. As the crystal structure of *P. putida* KT2440 ADI is still undetermined, the structural insights are not much clear. We addressed this issue by building homology model of *P. putida* KT2440 ADI. Molecular docking studies were carried out to explore the role of important catalytic residues in the interaction of enzyme-ligand complexes. Furthermore, various molecular interactions between the enzyme-ligand were studied by molecular dynamic simulations and correlated with the results obtained by the laboratory experiments.

* Corresponding author. Tel.: +91 172 2214682 85x2142; fax: +91 172 2214692.
E-mail addresses: mahi1709@gmail.com (M.D. Patil), vjrathod077@gmail.com (V.P. Rathod), umeshrsbihade@gmail.com (U.R. Bihade), ucbanerjee@niper.ac.in (U.C. Banerjee).

MATERIALS AND METHODS

Microorganism and cultivation conditions *P. putida* KT2440 was grown aseptically in a 14 L stirred-tank bioreactor (BioFlo 310; New Brunswick Scientific,

1389-1723/$ – see front matter
https://doi.org/10.1016/j.jbiosc.2018.07.021

Enfield, CT, USA) with a working volume of 8 L as previously reported (12). The broth was harvested after 24 h of fermentation and the cells were recovered by centrifugation (7000 × *g*, 20 min, 4°C). The cell pellet was washed twice with phosphate buffer (50 mM, pH 7.0) and used for the preparation of cell-free extract.

Purification of ADI from *P. putida* The cellmass slurry (200 g/L) of *P. putida* was disrupted by ultrasonication for 10 min as previously described (13). The debris was removed by centrifugation (7000 × *g*, 20 min at 4°C) and the supernatant was used for the purification of ADI. ADI activity was determined as previously described (12,14).

Initially, 20% (w/v) ammonium sulphate was adjusted in cell lysate with continuous stirring at 4°C. The solution was stirred for 2 h and then centrifuged for 30 min at 30,000 × *g*. The precipitate was discarded and ammonium sulphate was added to the supernatant so that the final concentration reached 40% (w/v) saturation. The solution was stirred for 2 h. The precipitate formed was discarded and ammonium sulphate was added to the supernatant so that the final concentration reached 80% (w/v) saturation. The resulting precipitate was collected by centrifugation for 30 min at 15,000 × *g*, resuspended in Tris buffer (20 mM, pH 8.0) and passed through 10 kDa centricon membrane (Millipore, Bedford, MA, USA).

The supernatant obtained after centrifugation was loaded on DEAE-Sepharose column (1.0 × 20 cm), saturated with 1 M NaCl in Tris buffer 20 mM, pH 8.0 and excess NaCl was removed by washing with Tris buffer (20 mM, pH 8.0) at a flow rate of 0.8 mL/min using fast protein liquid chromatography (Aktaprime, Amersham Biosciences, Uppsala, Sweden). ADI was eluted with the increasing gradient of NaCl (50–500 mM) in Tris buffer (20 mM, pH 8.0). Fractions were collected and analyzed for enzyme activity and protein content.

The eluted active fractions from the anion exchange chromatography were pooled and concentrated by filtration on a 100 kDa Centricon membrane (Millipore). The ultrafiltered solution was then loaded to phenyl-sepharose fast flow column (1.0 × 10 cm) (Amersham Biosciences), equilibrated with 1.7 M ammonium sulphate at 0.6 mL/min flow rate. ADI was eluted with decreasing concentration of ammonium sulphate.

Electrophoresis SDS-PAGE was performed on a 12% (w/v) polyacrylamide gel using Tris–glycine buffer system. The proteins were stained with 0.05% Coomassie Blue R-250 and the excess dye was washed out using destaining solution.

Determination of kinetic parameters of the purified ADI The kinetic parameters (K_m and V_{max}) of the purified enzyme were determined by double reciprocal Lineweaver–Burk plot. For this, enzyme activity was measured in the presence of increasing substrate concentration from 0.25 to 35 mM. The experiments were carried out in triplicate and average values are reported.

Determination of pH and temperature optima of the purified ADI Effect of pH and temperature on purified ADI was determined by incubating the enzyme with L-arginine in buffers of different pH (pH 4.0–8.0) and at different temperatures (4–50°C). ADI activity was determined in accordance with standard assay protocol and reported as relative activity. The maximum ADI activity was taken as 100%. The experiments were carried out in triplicate and average values are reported.

Effect of various chemical compounds on the purified ADI Influence of various chemical compounds (metal ions, reducing agents, sulphydryl agents, and surfactants) on the catalytic activity of ADI was determined by pre-incubating the enzyme with various compounds in 200 mM phosphate buffer (pH 6.0) for 15 min. Enzyme activity was determined by assaying the test solution under standard assay conditions and relative activity was expressed as a percentage of the activity in the absence of any test compound. The experiments were carried out in triplicate and average values are reported.

Substrate specificity of ADI toward structural analogues of arginine Specificity of substrate analogues towards *P. putida* ADI was determined by pre-incubating the enzyme with structural analogues of arginine in 200 mM phosphate buffer (pH 6.0) for 15 min. Enzyme activity was determined by assaying the test solution under standard assay conditions and relative activity was expressed as a percentage of the activity in the absence of any test compound. The experiments were carried out in triplicate and average values are reported.

Homology modeling of arginine deiminase from *P. putida* The FASTA sequence for arginine deiminase of *P. putida* KT2440 was retrieved from UniProt (http://www.uniprot.org/) (primary accession number Q88P52). The FASTA sequence on arginine deiminase contains 417 amino acids. The query sequence from the ADI was used to perform the basic local alignment search tool (BLAST) search on PDB database. Three structures were selected (PDB: 2A9G_D, 2ACI_A, 2ABR_A and 2AAF_A) as template for the model building on the basis of alignment length and the bit score obtained in the BLAST. The template with highest sequence similarity was then aligned according to their secondary structure using the MODLERER (align structure) and a sequence profile was generated by using the in-house database UniRef90 which is mainly used to produce the conserved residue based alignment. Further, to identify the conserved regions, a multiple alignment was carried out by aligning both templates and target structure. The multiple alignment structure was used for model construction using protocol Build homology model present in the Modeller9v6. The best model obtained from the protocol was subjected to the CHARMM for refining the model and minimized using Sybyl 7.1. The models obtained were checked for its dihedral distribution by Ramachandran plot. The ERRAT plot was examined to find out the geometric relationship between non-bonded contacts with C, N, O as a function of distance. Besides, the model was also verified by tools like PROCHECK, Varify 3D WHAT-IF and ProSA-web.

Molecular docking The developed model was selected as an initial structure for the protein preparation. The protein was prepared for bond orders, adding hydrogen bonds, finding overlaps and capping the terminals. The protein preparation was carried out at a pH 6.0. The resultant protein was then optimized and minimized to RMSD 0.30 Å using OPLS 2005 force field and was further used for the docking process. The structures of the substrates were drawn and minimized using Schrodinger 10.02 (Schrodinger, Cambridge, MA, USA). Substrates were then imported into the ligprep module and optimized using OPLS 2005 force field. All the substrates were subjected to all the possible states of ionization at pH 6.0 ± 0.2 using ionizer. The best-optimized structures out of 32 poses were selected. All the structures were saved in. mae format for further use. The prepared substrates were subjected to the docking procedure. The important catalytic residues were selected for the grid preparation and docking. The docking of the substrates was performed using the default parameters in Glide module (Schrodinger). All the substrates were docked using the standard precision (SP) method. The flexible docking was carried out for the generation of the ten different poses. The docked structures were analyzed based on the parameters like glide score, glide energy, and emodel score. The interaction diagramme was produced which mainly reported the hydrogen bonds, hydrophobic interactions and Pi–Pi interactions between substrates and the protein.

Molecular dynamic simulations The ligand-enzyme complexes obtained from molecular docking studies were further used for 10 ns molecular dynamic simulations using Desmond (Schrodinger v10.02) programme. The MD simulation calculations were done using the OPLS 2005 force field. The solvation of the complex was carried out using orthorhombic TIP3P water box (10Å × 10Å × 10 Å). The whole system was then neutralized by adding 0.15 M NaCl ions. The system was then minimized and run at a temperature of 310 K and pressure of 1.01325 bars.

Prime MM/GBSA free energy calculation The prime module was used for the prediction of the free binding energy of the substrates to protein. The complex and the separated protein and ligands were used for the calculation of the free energies. The novel energy model volume Bragg gratings (VBGs) were used as solvation model for optimizing the implicit solvent model and for the correction of the physics-based corrections of hydrogen bonding, π-π interactions, self-contact interactions and hydrophobic interactions.

RESULTS

Purification of ADI from *P. putida* Arginine deiminase from *P. putida* was purified to 13.3-fold with an yield of 11.69 % (Table 1) from the cellfree extract using two chromatographic procedures along with ammonium sulphate precipitation. Approximately 1.3-fold purification was achieved by ammonium sulphate precipitation with 41.4% yield. This fraction (147 U) was loaded on DEAE-sepharose with Tris buffer (pH 8.0, 20 mM) and eluted by gradient elution with 1 M sodium chloride in the same buffer. Partially purified protein fraction was achieved between 15% and 25% gradient of the elution buffer. A purification of 6.4-fold was achieved after this step. Partially purified ADI (147 U, from anion exchanger) was loaded on phenyl sepharose column with 1.7 M ammonium sulphate. Decreasing concentration of ammonium sulphate was used for elution. Purified protein fraction was achieved between the decreasing gradient of 0.4–0.1 M ammonium sulphate in the same buffer. The purified enzyme had specific activity of 70.3 U/mg and showed a prominent band on SDS-PAGE, suggesting that the enzyme preparation was significantly homogeneous (Fig. 1A).

TABLE 1. Purification of intracellular arginine deiminase from *Pseudomonas putida*.

Step	Enzyme activity (U)	Total protein (mg)	Specific activity (U/mg)	Yield (%)	Purification fold
Cell free extract	355	67	5.31	100	1
$(NH_4)_2SO_4$ precipitation	147	21.3	6.9	41.4	1.3
DEAE-Sepharose	102	3	34	28.73	6.4
Phenyl-sepharose	41.5	0.59	70.3	11.69	13.3

Determination of kinetic parameters of the purified ADI Kinetic parameters (the maximum reaction rate, V_{max}; Michaelis–Menten constant, K_m) of the purified ADI from *P. putida* were determined using L-arginine (0.25–35 mM) as substrate. The ADI activity increased linearly with the increasing substrate concentration up to 10 mM above which there was a substrate inhibition (Fig. 1B). Therefore, kinetic constants were determined within a substrate range of 0.25–10 mM. V_{max} and apparent K_m for the purified ADI were calculated to be 19.2 μmol/min·mg and 6 mM, respectively (Fig. 1C).

Determination of pH and temperature optima of the purified ADI The effect of pH on ADI activity was studied in different buffers (0.2 M) in the pH range of 4.0–8.0 (Fig. S1). The maximum enzyme activity was observed in phosphate buffer between the pH 6.0–6.4. ADI activity was stable over a pH range of 5.5–6.8. The enzyme retained approximately 15% of its activity at pH 7.4. ADI lost almost all of its activity below the pH 4.5 and beyond pH 7.4. The optimum temperature for catalysis was determined by measuring the enzyme activity at various temperatures over 10–50°C in phosphate buffer (pH 6.0, 0.2 M). ADI exhibited approximately 80% of its activity over a broad temperature range of 20–45°C, with an optimum temperature of 37°C (Fig. S1).

Effect of various chemical compounds Effect of various metal ions on ADI activity was found out by incubating the enzyme with salts of different metal ions (5–20 mM). The enzyme displayed high sensitivity towards thiol binding metal ions such as Zn^{2+}, Cu^{2+}, Hg^{2+} and Ag^{+} (relative activity: 19%, 15%, 5% and 0%, respectively) (Table S1). Such observations indicate the importance of thiol group in the catalytic activity. Though other metal ions did not significantly affect the enzyme activity, Fe^{2+} and Sn^{2+} caused a marked decrease in ADI activity (76% and 16%, respectively). This could possibly be attributed to the ability of these metal ions to form co–ordination complexes near the active site involving catalytically active thiol group. Reducing agents such as cysteine and sodium sulphite slightly decreased the ADI activity, while, glutathione and 2-mercaptoethanol had a positive effect on ADI activity (Table S2). Chemicals acting on sulfhydryl group, such as 5,5,-dithio-bis-(2-nitrobenzoic acid) (DTBN reagent) completely inhibited the ADI activity at 20 mM (Table S3). Most of the surfactants at higher concentration negatively affected the ADI activity, while Span 40 and alkanol marginally improved the % relative activity to 111 and 107, respectively (Table S4).

Substrate specificity of ADI The arginine deiminase can use some structural analogues of arginine as alternative substrates (15,16). The binding of these alternative substrates to ADI causes decrease in citrulline formation from arginine. A variety of structural analogues were used to study their effect on the inhibition of citrulline formation by ADI. Inhibition was studied by 15-min prior incubation of the enzyme with different concentrations (10–200 mM) of structural analogues, followed by the standard assay protocol. It was observed that canavanine had the highest affinity for ADI, followed by D-arginine and guanidine. Canavanine decreased the ADI activity up to 50% at its lowest concentration tested (10 mM), while D-arginine decreased the ADI activity up to ~4% at its highest tested concentration (200 mM). Inhibition of ADI activity suggested that these structural analogues of the substrate L-arginine had the varying affinity for *P. putida* ADI (Table 2).

Homology modeling The amino acid sequence of *P. putida* ADI protein was retrieved from UniProtKB (primary accession number: Q88P52). The FASTA sequence was retrieved and the protein sequence consisting of 417 amino acids was subjected to NCBI BLASTp search against Protein Data Bank (PDB) in order to find a template with suitable identity. Templates having PDB IDs 2A9G_A, 2ACI_A, 2ABR_A and 2AAF_A showed 84% sequence identities with the query sequence. Since PDB ID 2A9G_A showed higher sequence identity, higher cover of the query sequence (100%) and highest total score, it was selected as a template. The amino acid sequence was aligned with the template amino acid

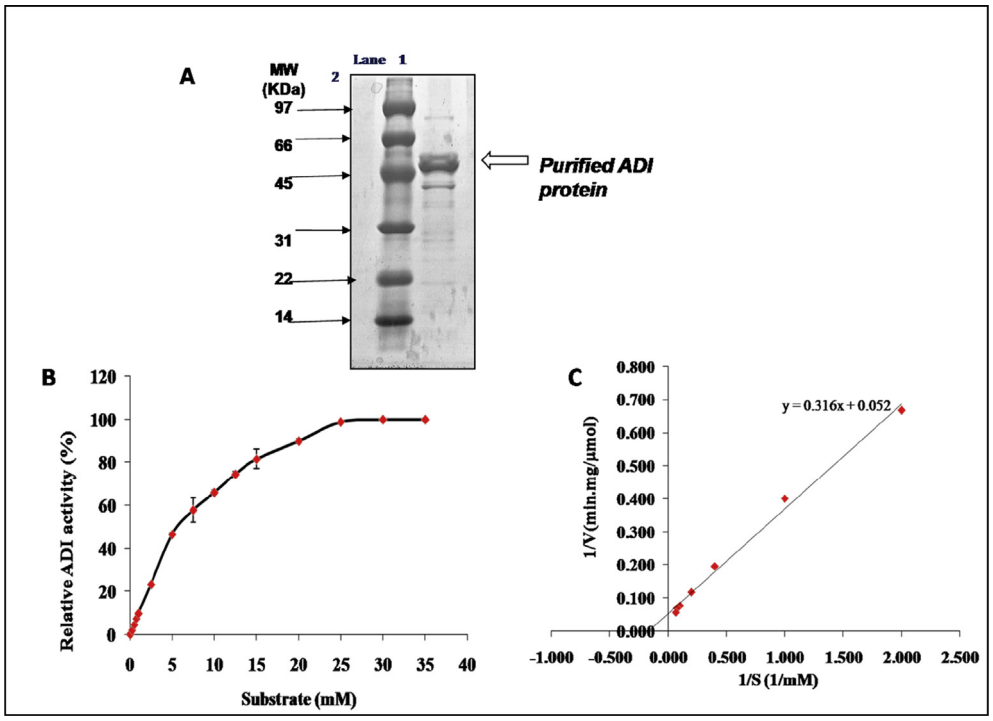

FIG. 1. (A) SDS-PAGE of the purified ADI from *Pseudomonas putida*. (B) Effect of substrate concentration and (C) estimation of kinetic constants of purified ADI by Lineweaver–Burk plot.

TABLE 2. Effect of varying concentration of substrate analogues on ADI activity.

Substrate analogue (mM)	Relative activity (%)[a]						
	10	20	40	60	80	100	200
D-Arginine	85.8	84.7	74.1	62.1	48.5	37.9	3.4
Agmatine	92.3	87.7	85.1	80.3	83.8	77.9	72.3
Putrescine	94.2	94.2	92.3	94.9	96.2	96.1	89.4
L-Canavanine	55.4	50.2	13.8	0.83	0.7	0.6	0
Homoarginine	97.7	94.0	91.9	87.3	78.0	75.5	75.0
3-Aminoalanine	96.6	94.4	92.3	90.6	89.0	89.3	72.5
L-Ornithine	88.5	86.9	80.8	79.5	84.2	82.0	76.4
Guanidine	90.8	85.5	82.6	80.3	76.3	75.7	65.5

[a] The ADI activity was expressed as a percentage of the activity in presence of L-arginine as a substrate.

TABLE 3. Docking scores and Glide energies for various substrate analogues and ADI complexes.

Substrate analogue	Docking score (kcal/mol)	Glide score (kcal/mol)
L-Arginine	−7.72	−7.72
D-Arginine	−7.46	−7.46
Agmatine	−6.56	−6.56
Putrescine	−5.74	−5.74
L-Canavanine	−7.51	−7.51
Homoarginine	−5.33	−5.33
3-Aminoalanine	−4.10	−5.88
L-Ornithine	−6.60	−6.60
Guanidine	−6.35	−6.35

using ClustalW. Fig. S2 shows the alignment of the query sequence with the template sequence.

Model building and refinement The initial model of *P. putida* ADI was built using the Modeller9v6 program. Initially 100 models were built and models were evaluated using DOPE score, Ramachandran and ERRAT plot. Ramachandran plot for model number 30 showed that 97.8% (406 out of 417) amino acids lie in the favored region and only 2 amino acids lie in the outlier region (Fig. S3). Moreover, ERRAT plot showed the value of 89.578. Therefore, this model was finalized as the homology model of the ADI from *P. putida* KT2440.

Molecular docking The developed model (Fig. 2) was selected as an initial structure for molecular docking. Table 3 depicts the results of docking studies. Moreover, there was a positive correlation between the docking scores and the experimental inhibition of ADI activity in the presence of these substrate analogues. The higher negative docking scores suggest that the compound is more potent. For instance, L-arginine is having highest affinity for ADI and its docking score was found to be −7.7 kcal/mol. Moreover, interaction diagrams showing the important interactions taking place among the substrate analogues and the ADI are shown in Fig. 3.

Molecular dynamic simulations The complex structures obtained for all the substrate analogues from molecular docking studies were further used for the 10-ns Molecular dynamics simulation studies using Desmond (Schrodinger v10.02). RMSD not only measures the average change in displacement of atoms for a particular frame with respect to a reference frame but also give insights into its structural conformation throughout the simulation. The smaller deviation in the RMSD (1–3 Å) is acceptable for small, globular proteins, while changes much larger than that indicate the conformational instability of the protein during simulation (17,18). As shown in Fig. S4, RMSD values for protein backbone were within an acceptable ranges (1–3 Å), suggesting that the protein was stable during the simulations. Similarly, if the values observed are significantly larger than the RMSD of the protein, then it is likely that the ligand has diffused away from its initial binding site. In the present study, RMSDs for protein-ligand complexes were very small, suggesting that the protein ligand complexes were stable throughout the simulation.

Furthermore, we analyzed the different molecular interaction pattern along the 10-ns simulation time to examine the effect of these molecular interactions on the ligand-ADI complexes. Hydrogen bonds are assumed to be formed if the distance between donor and the acceptor is within 5 Å (19). Interaction between a hydrophobic amino acid and an aromatic or aliphatic group on the ligand forms hydrophobic contacts (20), while two oppositely charged atoms that are within 3.7 Å of each other form Ionic/polar interactions. Water bridges are hydrogen-bonded

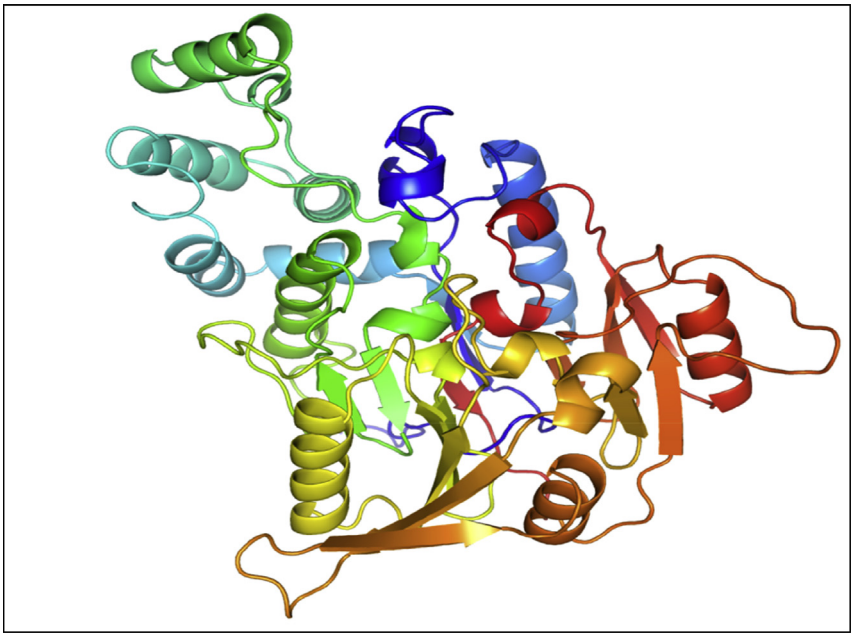

FIG. 2. Homology model of ADI from *Pseudomonas putida*.

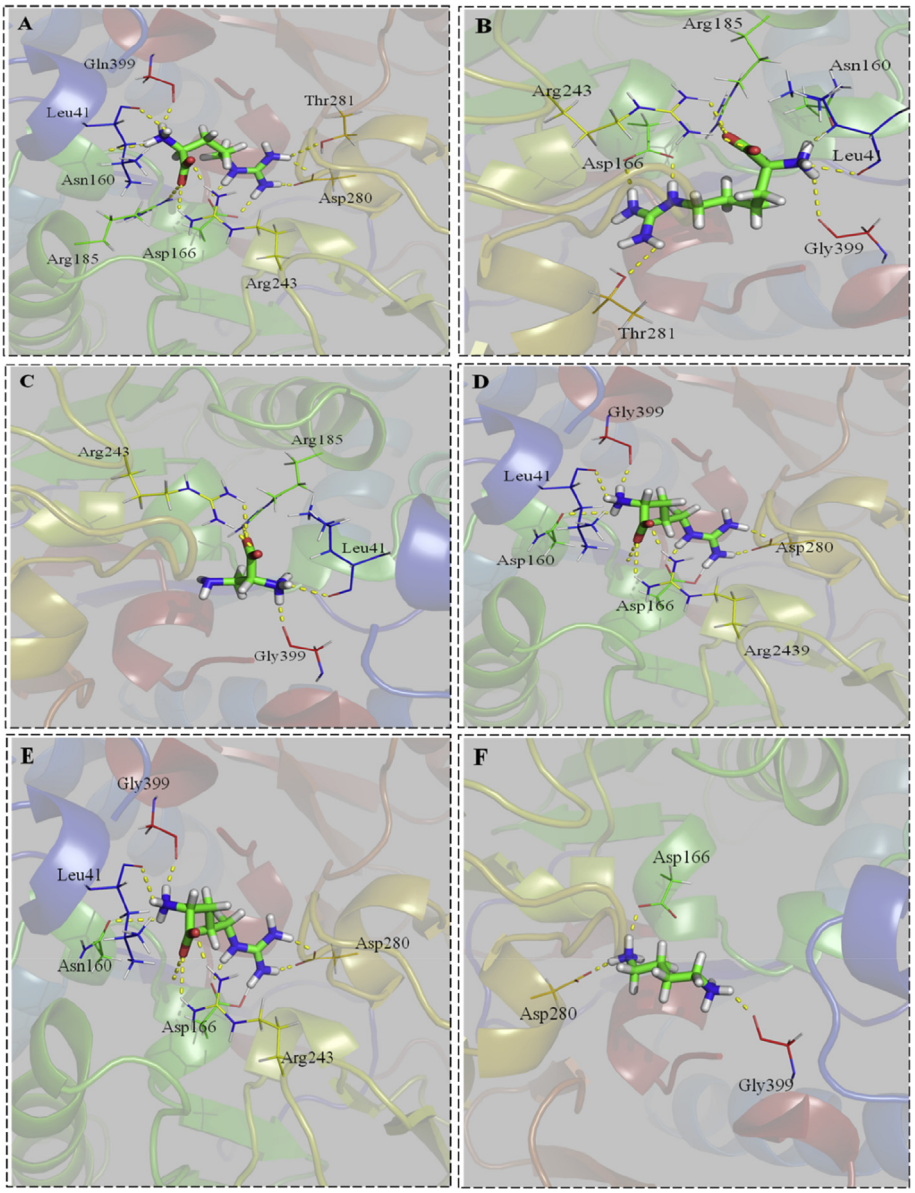

FIG. 3. Interaction diagram and docking poses for substrate analogues. (A) L-Arginine, (B) homoarginine, (C) aminoalanine, (D) agmatine, (E) D-arginine, (F) putrescine, (G) canavanine, (H) ornithine, and (I) guanidine.

protein-ligand interactions mediated by water molecule (21). As can be seen in Fig. 4, the pattern and extent of these molecular interactions were distinctive for each of the substrate analogue. The difference in the extent and type of molecular interactions can be speculated as a molecular mechanism for the differential affinity of substrate analogues towards *P. putida* ADI. The binding free energies were calculated to analyze the molecular interactions of the substrate analogues and ADI. The various components of binding energies for all the substrate–protein complexes are shown in Table 4.

DISCUSSION

Arginine deiminase is a promising drug modality against the hepatocellular carcinomas, melanomas and other arginine auxotrophic tumor types (1,22,23). In the present study, ADI from *P. putida* KT2440 was purified and characterized. Also, the data acquired from the *in silico* studies would be advantageous for further investigation on the catalytic properties of ADI from *P. putida*.

ADI from various microorganisms has been characterized and reported in the literature. Specific activity of a purified enzyme is a characteristic feature and is a function of the substrates used. In the present study, the purified ADI from *P. putida* exhibited the maximum reaction rate (V_{max}) of 19.2 μmol/min·mg and K_m of ~6 mM. A range of ADI activities from 0.1 to 143 U/mg from various microbial species are reported in literature (9). For instance, Monstadt and Holldorf (24) have reported the specific activity of ADI as 5.4 U/mg from *Halobacterium saliniarium*. The highest specific activity of ADI (143 U/mg) has been reported from *Lactobacillus lactis* (25). The specific ADI activities of 44.5 and 35 U/mg from *Mycoplasma arginini* and *Mycoplasma hominis*, respectively are also reported in the literature (26,27). Similarly, K_m is an important parameter that depicts the affinity of the enzyme towards its substrate. K_m values of 0.2–8.7 mM have been reported for the ADIs from various microorganisms (8). The K_m values reported for *P. plecoglossicida* and *L. lactis* are 2.88 and 8.7 mM, respectively.

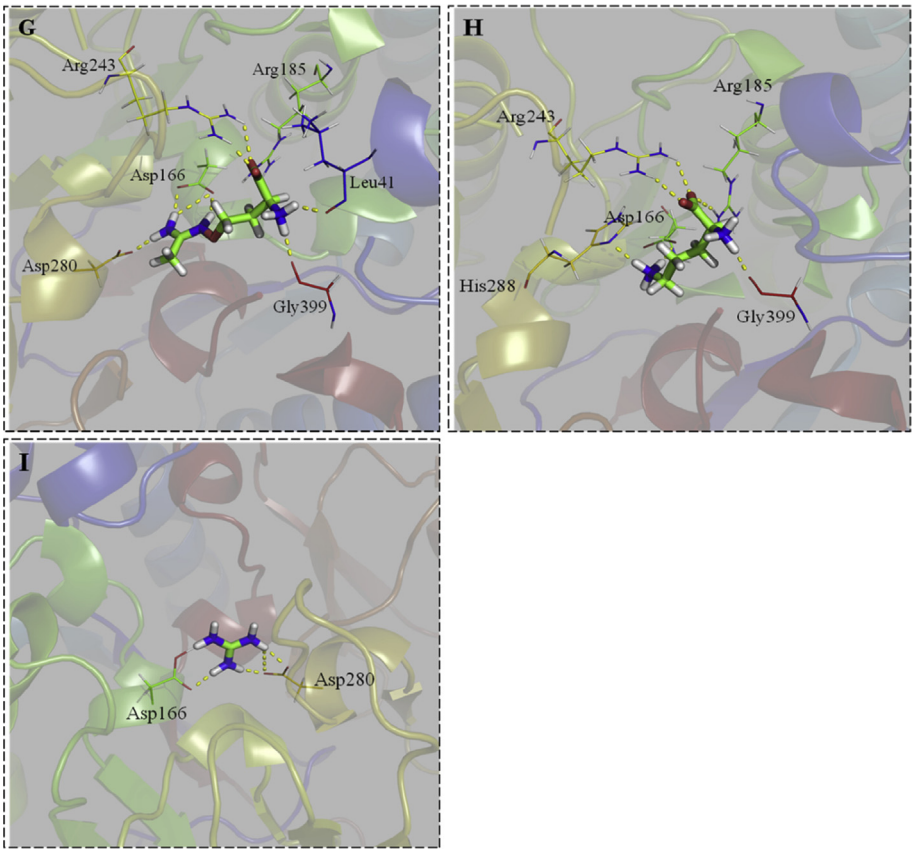

FIG. 3. (*continued*).

However, the K_m value for ADI from *P. putida* in our study (6 mM) is slightly higher than that of previously reported values in *Pseudomonas* sp. (9). The sensitivity of the various assay methods may be one of the reasons for the difference in K_m values. The affinity of an enzyme obtained from various sources obviously depends on the type of organism, environmental conditions for the cultivation and purity of the enzyme.

The effect of temperature and pH was evaluated on the purified ADI from *P. putida*. ADI exhibited an optimal pH range of 6.0—6.4 for its maximal catalytic activity. Both on the acidic and alkaline pH conditions, the ADI activity had drastically reduced. This result was in good agreement with the previously reported literature (9). The optimum pH of arginine deiminase from *P. putida* and *M. hominis* has been reported to pH 6.0 (27,28). The optimum pH values for the ADIs from the various microbial species are found to vary significantly from pH 5.0 to 7.4 (29) and amino acid residue at the position 404 has been reported as crucial for the differences in the pH optima (8,29). It has been reported that the ADI having His 404 exhibits the acidic pH optima, as in the case of *Burkholderia mallei* (30) and *P. aeruginosa* (16), while on the other hand, as in cases of *Bacillus cereus* (30) and *M. hominis* (31), the optimum pH has been demonstrated to be higher with the presence of arginine at position 404. Differential hydrogen bonding network involving these residues has been proposed as a catalytic mechanism for the differences in the optimum pH values (29). Previously reported studies in *P. putida* have reported the optimum temperature of ADI as 50°C (28). The optimum temperature for ADI in the present study was found to be 37°C.

The *in silico* study was aimed towards gaining the structural insights for the differential affinities of the structural analogues of arginine towards ADI. To understand the binding mode of structural analogues, we have carried out the molecular modeling that is, molecular docking and molecular dynamics. The study of molecular docking revealed the critical importance of residues Arg 243, Asp 166, Asp 280, Gly 299 and His 278. The docking study also showed that the molecular interactions for D-arginine and canavanine had similar interactions as that of L-arginine. L-Arginine was strongly bound by strong hydrogen bonds. In accordance with the previous reports (32), two hydrogen bonds were formed each by Asp166 and Asp280. Moreover, other hydrogen bonds were formed such as, two between Arg 243 and oxygens of carboxylate group, one between Arg 185 and carboxylate group of L-arginine, one each between Asn 160, Gly 399 and amino group of the substrate (Fig. S5). Molecular docking further revealed that formation of all these hydrogen bonds was consistent in D-arginine and canavanine. Only the hydrogen bond between Asn160 and amino group of L-arginine was observed exclusively for L-arginine. It was also observed that the bond lengths for all the hydrogen bonds between these substrates and protein ranged from 1.4 to 2.6 Å, indicating the stronger interactions. The common molecular interactions by the residues Asp166, Asp280, Gly399 for all the substrate analogues indicated the importance of these residues for the catalytic binding of the substrates. Also, L-arginine, D-arginine and canavanine showed the common hydrophobic interactions with residues Cys 405, Leu 41 and Phe 163. Present experimental studies also showed that canavanine had the strongest affinity towards ADI, as it diminished ADI activity up-to its half at the concentration of 20 mM. Docking studies of canavanine also showed additional ionic interactions with the residues Asn160, Asn 359, Thr281 and His278. It has also been reported in literature that L-canavanine is a time-controlled mechanism-based inhibitor of *Pseudomonas aeruginosa* arginine deiminase (33).

Two important substrate binding residues, i.e., Asp280 and Asp166 participate in stabilizing the substrate guanidinium group. Though both of these residues are required for catalytic conversion

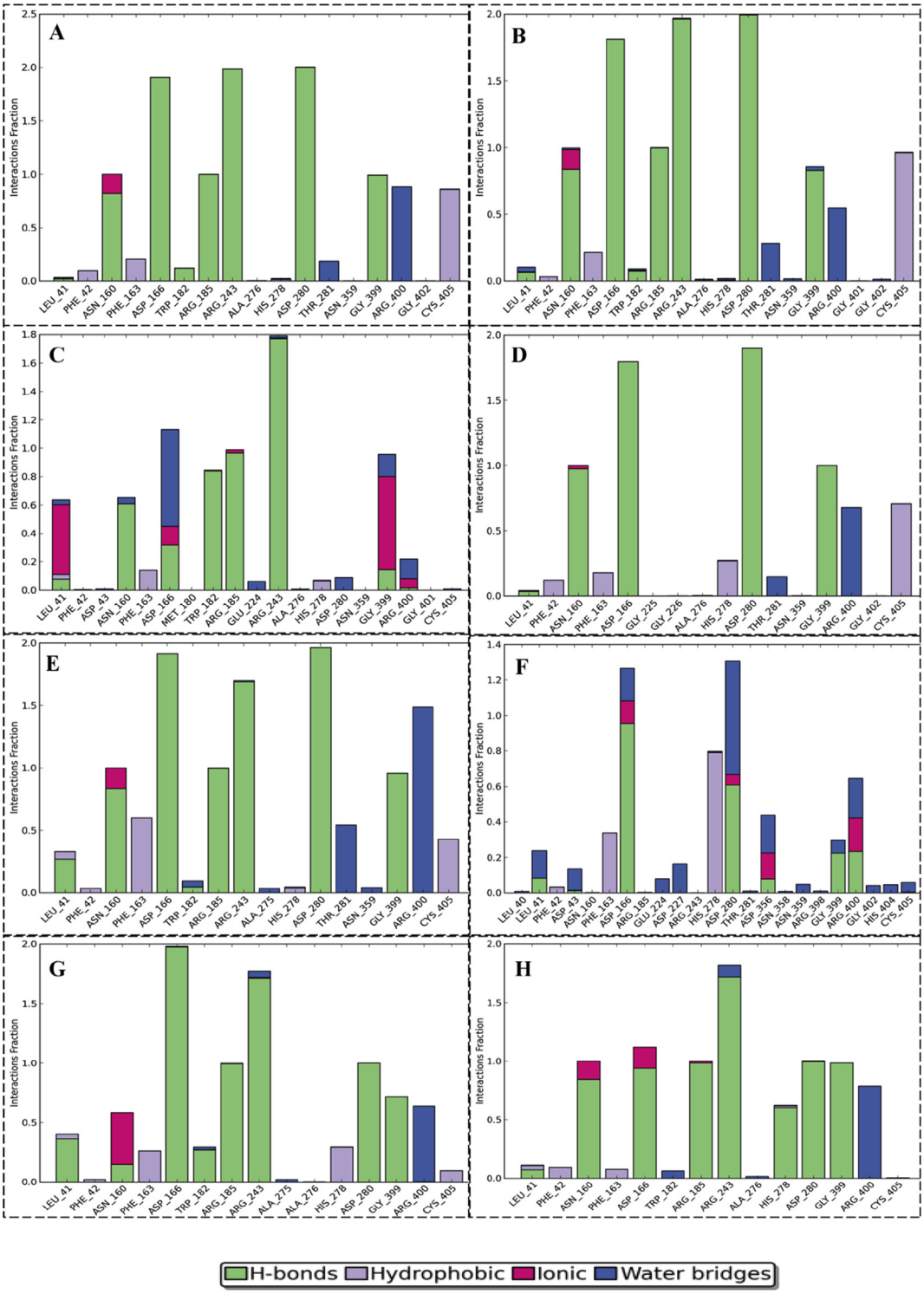

FIG. 4. Molecular interactions of arginine deiminase with substrate analogues in the molecular dynamics simulations. (A) L-Arginine, (B) homoarginine, (C) aminoalanine, (D) agmatine, (E) D-arginine, (F) putrescine, (G) canavanine, and (H) ornithine.

of arginine to citrulline, the exact roles of Asp166 and Asp280 have been reported to be different (5). The main function of Asp166 is countering the charge of the substrate guanidinium group, whereas the primary role of Asp280 is in the enhancement of the electrophilicity of the substrate guanidinium Cζ atom and activation of the water molecule (5,29,30).

The biological studies of the micro- and macromolecules can be well illustrated using molecular modeling studies (29,33–37). Molecular dynamics conditions could be used to investigate ADI-substrate interactions. We performed the molecular dynamics of nine structural analogues of arginine for 10 ns to examine the complex stability. The binding conformations of the complexes were analyzed under the dynamic state. The trajectories formed in molecular dynamics were used to inspect the molecular interactions between the protein and substrate. The trajectory analysis for the RMSDs of protein backbones illustrated that all the

TABLE 4. Binding energies and their components for various substrate analogues and ADI complexes.

Substrate	ΔG_{bind} (kcal/mol)	$\Delta G_{Covalent}$ (kcal/mol)	ΔG_{Hbond} (kcal/mol)	ΔG_{Lipo} (kcal/mol)	ΔG_{vdw} (kcal/mol)
L-Arginine	−77.96	3.00	−13.16	−15.08	−23.83
D-Arginine	−78.83	2.09	−12.84	−15.50	−23.93
Agmatine	−67.70	2.33	−10.82	−15.44	−18.79
Putrescine	−31.46	1.65	−2.41	−11.54	−8.33
L-Canavanine	−59.24	2.45	−5.85	−13.56	−23.91
Homoarginine	−55.31	8.74	−12.77	−20.03	1.34
3-Aminoalanine	−22.33	0.73	−3.01	−7.03	−16.75
L-Ornithine	−43.71	1.23	−3.98	−13.37	−21.81
Guanidine	−49.30	1.27	−12.15	−2.53	−6.36

systems got stabilized after 5 ns within the range of 0.5 Å, where all showed a slight fluctuation in the initial phase of the simulation and then got stabilized (Fig. S4). This suggests that the presence of substrate analogues inside the catalytic cavity of ADI did not have significant effect on the stability of backbone. In the case of putrescine, protein backbone showed the maximum fluctuation and got stabilized after 5 ns. Experimental studies also demonstrated that putrescine and 3-aminoalanine have the less affinity towards the ADI compared to other substrates (Table 2). This was consistent with the results of docking (Table 3), trajectory analysis for RMSD (Fig. 4) and binding energies (Table 4). Agmatine and putrescine exhibited marginally higher RMSD fluctuations indicating their lower binding affinity with ADI. Molecular dynamic simulations of the L-arginine with the built homology model of ADI also corroborated the formation of strong hydrogen bonds by residues Asn 160, Asp 166, Arg 185, Arg 243, Asp 280 and Gly 399. These hydrogen bonds were preserved in the case of D-arginine and canavanine. However, some of these hydrogen bonds were not observed in other substrate analogues indicating their lower affinity towards ADI (Fig. S5). For instances, hydrogen bonds with Arg185 and Arg243 in agmatine and Asn160, Arg185, Arg243 in putrescine were not formed as that of in L-arginine, D-arginine and canavanine. Moreover, the interaction fraction of hydrogen bonds in these substrate analogues was smaller, corroborating the weaker interaction of these substrate analogues with the homology model of ADI (Fig. 4). Similarly, agmatine and putrescine have been reported to exhibit lower affinities towards arginine deiminase from the primitive eukaryote *Giardia intestinalis* (15). The experimental data also demonstrated the highest affinity of canavanine followed by D-arginine. The affinities for other substrate analogues were comparable (Table 2).

Calculations of the substrate binding energies illustrated the respective binding affinity for the substrates. D-arginine and L-arginine showed the highest binding affinity (ΔG_{bind}) compared to all the substrates. The same result was also supported by the outcomes of binding energies for van der Waal interactions (ΔG_{vdw}) (Table 4). It can be concluded that the binding energies ΔG_{bind} and ΔG_{vdw} play crucial role in the differential affinities of the substrate analogues towards *P. putida* ADI.

To conclude, arginine deiminase from *P. putida* was purified to homogeneity using a combination of precipitation and chromatographic techniques. The effect of various chemical compounds on the purified ADI was evaluated. The affinities of the various structural analogues of arginine towards ADI were studied by the inhibition assays. Experimental studies showed that canavanine and D-arginine had strongest affinity towards ADI. To study the molecular interactions of these substrate analogues and the enzyme, homology model of the ADI was build up and validated using Ramachandran and ERRAT plots. The developed homology model was used for the molecular docking of the substrate analogues. Docking studies corroborated the experimental results, as docking and Glide scores were maximum for L-arginine, followed by canavanine and D-arginine. The ADI-substrate complexes from molecular docking studies were further used for the molecular dynamic (MD) simulations. MD simulations demonstrated the crucial role of the following residues Arg 243, Asp 166, Asp 280, Gly 299 and His 278 in the formation of molecular interactions of the substrates and ADI. Also, it was concluded that the variations in the molecular interactions are responsible for the differential affinities of various substrate analogues towards ADI from *P. putida*. It is being intensely believed that the combination of experimental and *In silico* studies performed herein are potentially helpful for the scientific community in the generation of active site mutants and the directed evolution approaches for the modification of ADI as a more potent anti-cancer modality.

Supplementary data related to this article can be found at https://doi.org/10.1016/j.jbiosc.2018.07.021.

ACKNOWLEDGMENTS

MDP gratefully acknowledges Department of Biotechnology (DBT), New Delhi, India, for the award of Senior Research Fellowship. Authors are thankful to Mr. Mukesh Kumar, Mr. Manoj Dev for the technical assistance. Authors also gratefully acknowledge Professor Manfred Zinn, Laboratory for Biomaterials, Empa-Swiss Federal Laboratories for Materials Science and Technology, Switzerland for the kind gift of *Pseudomonas putida* KT2440 strain. This research did not receive any specific grant from funding agencies in the public, commercial, or not-for-profit sectors. All the authors declare that they have no competing interests.

References

1. **Patil, M. D., Bhaumik, J., Babykutty, S., Banerjee, U. C., and Fukumura, D.:** Arginine dependence of tumor cells: targeting a chink in cancer's armor, Oncogene, **35**, 4957–4972 (2016).
2. **Yamamoto, K., Sato, T., Tosa, T., and Chibata, I.:** Continuous production of L-citrulline by immobilized *Pseudomonas putida* cells, Biotechnol. Bioeng., **16**, 1589–1599 (1974).
3. **Patil, M. D., Dev, M. J., Shinde, A. S., Bhilare, K. D., Patel, G., Chisti, Y., and Banerjee, U. C.:** Surfactant-mediated permeabilization of *Pseudomonas putida* KT2440 and use of the immobilized permeabilized cells in biotransformation, Process Biochem., **63**, 113–121 (2017).
4. **Ni, Y., Schwaneberg, U., and Sun, Z.:** Arginine deiminase, a potential anti-tumor drug, Cancer Lett., **261**, 1–11 (2008).
5. **Galkin, A., Kulakova, L., Sarikaya, E., Lim, K., Howard, A., and Herzberg, O.:** Structural insight into arginine degradation by arginine deiminase, an antibacterial and parasite drug target, J. Biol. Chem., **279**, 14001–14008 (2004).
6. **Galkin, A., Lu, X., Dunaway-Mariano, D., and Herzberg, O.:** Crystal structures representing the Michaelis complex and the Thiouronium reaction intermediate of *Pseudomonas aeruginosa* arginine deiminase, J. Biol. Chem., **280**, 34080–34087 (2005).
7. **Liu, Y.-M., Sun, Z.-H., Ni, Y., Zheng, P., Liu, Y.-P., and Meng, F.-J.:** Isolation and identification of an arginine deiminase producing strain *Pseudomonas plecoglossicida* CGMCC2039, World J. Microbiol. Biotechnol., **24**, 2213–2219 (2008).
8. **Ni, Y., Liu, Y., Schwaneberg, U., Zhu, L., Li, N., Li, L., and Sun, Z.:** Rapid evolution of arginine deiminase for improved anti-tumor activity, Appl. Microbiol. Biotechnol., **90**, 193–201 (2011).
9. **Zhu, L., Tee, K. L., Roccatano, D., Sonmez, B., Ni, Y., Sun, Z.-H., and Schwaneberg, U.:** Directed evolution of an antitumor drug (arginine deiminase PpADI) for increased activity at physiological pH, Chembiochem, **11**, 691–697 (2010).
10. **Zhu, L., Verma, R., Roccatano, D., Ni, Y., Sun, Z.-H., and Schwaneberg, U.:** A potential antitumor drug (Arginine Deiminase) reengineered for efficient operation under physiological conditions, Chembiochem, **11**, 2294–2301 (2010).
11. **Jiang, H., Guo, S., Xiao, D., Bian, X., Wang, J., Wang, Y., Zhou, H., Cai, J., and Zheng, Z.:** Arginine deiminase expressed *in vivo*, driven by human telomerase reverse transcriptase promoter, displays high hepatoma targeting and oncolytic efficiency, Oncotarget, **8**, 37694–37704 (2017).
12. **Patil, M. D., Shinde, K. D., Patel, G., Chisti, Y., and Banerjee, U. C.:** Use of response surface method for maximizing the production of arginine deiminase by *Pseudomonas putida*, Biotechnol. Rep., **10**, 29–37 (2016).
13. **Patil, M. D., Dev, M. J., Tangadpalliwar, S., Patel, G., Garg, P., Chisti, Y., and Banerjee, U. C.:** Ultrasonic disruption of *Pseudomonas putida* for the release of

arginine deiminase: kinetics and predictive models, Bioresour. Technol., **233**, 74–83 (2017).
14. **Patil, M. D., Patel, G., Surywanshi, B., Shaikh, N., Garg, P., Chisti, Y., and Banerjee, U. C.:** Disruption of *Pseudomonas putida* by high pressure homogenization: a comparison of the predictive capacity of three process models for the efficient release of arginine deiminase, AMB Expr., **6**, 84 (2016).
15. **Knodler, L. A., Sekyere, E. O., Stewart, T. S., Schofield, P. J., and Edwards, M. R.:** Cloning and expression of a prokaryotic enzyme, arginine deiminase, from a primitive eukaryote *Giardia intestinalis*, J. Biol. Chem., **273**, 4470–4477 (1998).
16. **Lu, X., Li, L., Wu, R., Feng, X., Li, Z., Yang, H., Wang, C., Guo, H., Galkin, A., Herzberg, O., and other 3 authors:** Kinetic analysis of *Pseudomonas aeruginosa* arginine deiminase mutants and alternate substrates provides insight into structural determinants of function, Biochemistry, **45**, 1162–1172 (2006).
17. **Nosé, S.:** Constant temperature molecular dynamics methods, Prog. Theor. Phys. Suppl., **103**, 1–46 (1991).
18. **Karplus, M. and McCammon, J. A.:** Molecular dynamics simulations of biomolecules, Nat. Struct. Mol. Biol., **9**, 646 (2002).
19. **Perrin, C. L. and Nielson, J. B.:** "Strong" hydrogen bonds in chemistry and biology, Annu. Rev. Phys. Chem., **48**, 511–544 (1997).
20. **Karplus, P. A.:** Hydrophobicity regained, Protein Sci., **6**, 1302–1307 (1997).
21. **Mattos, C.:** Protein–water interactions in a dynamic world, Trends Biochem. Sci., **27**, 203–208 (2002).
22. **Han, R.-Z., Xu, G.-C., Dong, J.-J., and Ni, Y.:** Arginine deiminase: recent advances in discovery, crystal structure, and protein engineering for improved properties as an anti-tumor drug, Appl. Microbiol. Biotechnol., **100**, 4747–4760 (2016).
23. **Patil, M. D., Shinde, A. S., Dev, M. J., Patel, G., Bhilare, K. D., and Banerjee, U. C.:** Combined effect of attrition and ultrasound on the disruption of *Pseudomonas putida* for the efficient release of arginine deiminase, Biotechnol. Prog., **34**, 1185–1194 (2018).
24. **Monstadt, G. M. and Holldorf, A. W.:** Arginine deiminase from *Halobacterium salinarium*: purification and properties, Biochem. J., **273**, 739–745 (1990).
25. **Kim, J.-E., Jeong, D.-W., and Lee, H. J.:** Expression, purification, and characterization of arginine deiminase from *Lactococcus lactis* ssp. *lactis* ATCC 7962 in *Escherichia coli* BL21, Protein Expr. Purif., **53**, 9–15 (2007).
26. **Takaku, H., Takase, M., Abe, S.-I., Hayashi, H., and Miyazaki, K.:** *In vivo* antitumor activity of arginine deiminase purified from *Mycoplasma arginini*, Int. J. Cancer, **51**, 244–249 (1992).
27. **Takaku, H., Matsumoto, M., Misawa, S., and Miyazaki, K.:** Anti-tumor activity of arginine deiminase from *Mycoplasma arginini* and its growth-inhibitory mechanism, Jpn. J. Cancer, **86**, 840–846 (1995).
28. **Shibatani, T., Kakimoto, T., and Chibata, I.:** Crystallization and properties of L-arginine deiminase of *Pseudomonas putida*, J. Biol. Chem., **250**, 4580–4583 (1975).
29. **Ding, H., Liu, H., Yin, Y., Ding, Y., Jia, Y., Chen, Q., Zou, G., and Zheng, Z.:** Insights into the modulation of optimum pH by a single histidine residue in arginine deiminase from *Pseudomonas aeruginosa*, Biol. Chem., **393**, 1013–1024 (2012).
30. **Li, L., Li, Z., Wang, C., Xu, D., Mariano, P. S., Guo, H., and Dunaway-Mariano, D.:** The electrostatic driving force for nucleophilic catalysis in L-Arginine deiminase: a combined experimental and theoretical study, Biochemistry, **47**, 4721–4732 (2008).
31. **Wei, Y., Zhou, H., Sun, Y., He, Y., and Luo, Y.:** Insight into the catalytic mechanism of arginine deiminase: functional studies on the crucial sites, Proteins, **66**, 740–750 (2007).
32. **Wang, C., Xu, D., Zhang, L., Xie, D., and Guo, H.:** Molecular dynamics and density functional studies of substrate binding and catalysis of arginine deiminase, J. Phys. Chem., **B111**, 3267–3273 (2007).
33. **Lu, X., Li, L., Feng, X., Wu, Y., Dunaway-Mariano, D., Engen, J. R., and Mariano, P. S.:** L-Canavanine is a time-controlled mechanism-based inhibitor of *Pseudomonas aeruginosa* arginine deiminase, J. Am. Chem. Soc., **127**, 16412–16413 (2005).
34. **Xu, X. Q., Han, W., Wu, X. B., Xie, Y., Lin, J., and Chen, Q. X.:** Inactivation kinetics and conformation change of *Hypocreaorientalis* β-glucosidase with guanidine hydrochloride, J. Biosci. Bioeng., **124**, 143–149 (2017).
35. **Kawabata, T., Oda, M., and Kawai, F.:** Mutational analysis of cutinase-like enzyme, Cut 190, based on the 3D docking structure with model compounds of polyethylene terephthalate, J. Biosci. Bioeng., **124**, 28–35 (2017).
36. **Li, J., Wang, C., Hu, D., Yuan, F., Li, X., Tang, S., and Wu, M.:** Engineering a family 27 carbohydrate-binding module into an *Aspergillus usamii* β-mannanase to perfect its enzymatic properties, J. Biosci. Bioeng., **123**, 294–299 (2017).
37. **Watanabe, F., Yu, F., Ohtaki, A., Yamanaka, Y., Noguchi, K., Odaka, M., and Yohda, M.:** Improvement of enantioselectivity of the B-type halohydrin hydrogen-halide-lyase from *Corynebacterium* sp. N-1074, J. Biosci. Bioeng., **122**, 270–275 (2016).